Highlights from the STAR experiment

Alexey Aparin[1,*] for the STAR collaboration

[1]Joint Institute for Nuclear Research

Abstract. We present an overview of the recent results obtained by the STAR Collaboration at RHIC. We report the beam energy dependence of directed flow of strange particles. These results support the assumption, that directed flow is formed before hadronization and observed particles are formed via coalescence of constituent quarks. First evidence of a non-zero directed flow of D^0 meson is reported. We present the precision measurement of elliptic flow of D^0 meson and the first measurement of Λ_c baryon in Au+Au collisions at $\sqrt{s_{NN}}$ = 200 GeV, which suggests thermalization of charm quarks. We report results of global Λ polarization measurements in Au+Au collisions, together with the investigation of polarization dependence of centrality and transverse momentum p_T. Results from the STAR fixed-target program show good agreement with previously obtained results. A precise measurement of the ${}^3_\Lambda H$ lifetime is presented. Mesonic decay modes are used to reconstruct the ${}^3_\Lambda H$ from Au+Au collisions. The measured lifetime is about 50% shorter than the one of a free Λ, indicating strong hyperon-nucleon interaction in the hypernucleus system. Finally, we give an outlook to detector upgrades for the Beam Energy Scan phase II.

1 Azimuthal anisotropy measurements

One of the most important observables in heavy-ion experiments is the azimuthal anisotropic flow [1] that is usually quantified by the Fourier coefficients of the azimuthal distribution of the final state particles relative to the collision symmetry planes $Ed^3N/dp^3 = 1/2\pi \cdot d^2N/p_t dp_t d\eta \cdot (1 + \Sigma 2 v_n cos[n(\phi - \Psi_n)])$. The first-order coefficient, called the directed flow, is argued to be sensitive to the equation of state of the matter, and could serve as a possible signature of the QGP phase transition. STAR has recently performed directed flow measurements at mid-rapidity for $\Lambda, \bar{\Lambda}, K^{\pm}, K_s^0$, and ϕ at $\sqrt{s_{NN}}$ = 7.7, 11.5, 14.5, 19.6, 27, 39, 62.4 and 200 GeV in Au+Au collisions. Results show good sensitivity for testing a picture where flow is assumed to be formed before hadron formation and the observed particles are assumed to form via coalescence of constituent quarks. Figure 1 represents $v_1(y)$ for indicated particles at two centralities. One can see that within errors, the plotted species have a near linear $v_1(y)$ over the acceptance of the STAR detector.

Directed flow slope dv_1/dy versus beam energy for $\Lambda, \bar{\Lambda}, K^{\pm}, K_s^0, \phi$ was also studied [2] and compared with the data for $\pi^{\pm}, p$ and $\bar{p}$ [3]. Combined data for the ten particle species available allow a detailed investigation of constituent quark v_1. Obtained results support the assumption called the coalescence sum rule [4]. In this scenario the directed flow v_1 is

*e-mail: aparin@jinr.ru

formed at the pre-hadronic stage, specific types of quarks have the same directed flow and the detected hadrons are formed via coalescence.

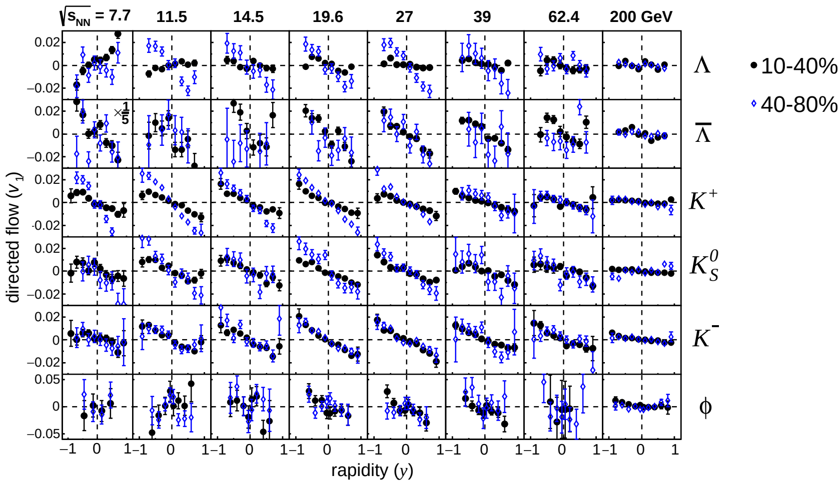

Figure 1. Directed flow as a function of rapidity for the six indicated particle species in 10-40% (black) and 40-80% (blue) central Au+Au collisions at $\sqrt{s_{NN}}$ = 7.7 to 200 GeV. The error bars include statistical uncertainties only. All panels for species other than ϕ use the same v_1 scale with the exception of $\bar{\Lambda}$ at $\sqrt{s_{NN}}$ = 7.7 GeV, where v_1 magnitudes are exceptionally large and require the measurements to be divided by five.

Direct measurements of charmed hadrons require very good vertex detector due to their very short lifetimes. STAR had installed the Heavy Flavor Tracker (HFT) [5], the MAPS-based vertex detector for run years 2014-2016. This allowed to perform precise measurements of flow for heavy flavor particles [6].

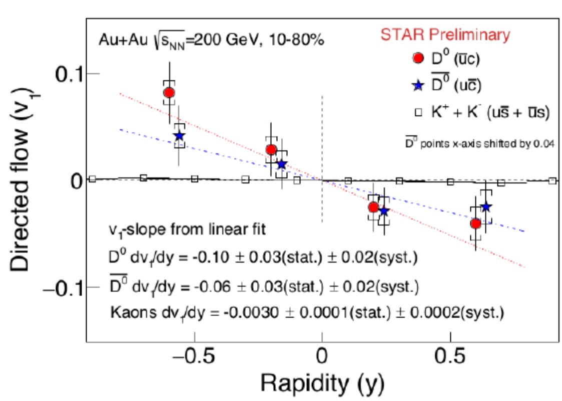

Figure 2. Directed flow as a function of rapidity for D^0 mesons in 10–80% centrality Au+Au collisions at $\sqrt{s_{NN}}$ = 200 GeV compared with directed flow of $K^+ + K^-$. Data points for $\bar{D}^0$ are slightly shifted for visibility.

Figure 2 shows the first measurement of directed flow for charmed meson D^0 produced in Au-Au collisions for 10–80% centrality. It is clear that within the errors value of $v_1(y)$ is non-zero and follows the linear trend obtained previously for light particle sector. The second harmonic of the charmed meson D^0 was recently studied using data from run years 2014 and 2016. The measured D^0 v_2 in 0–80% centrality Au+Au collisions can be described by a viscous hydrodynamic calculation for transverse momentum p_T less than 4GeV/c. The D^0 v_2 as a function of transverse kinetic energy ($m_T - m_0$, where $m_T = \sqrt{p_T^2 + m^2}$) is consistent with that of light mesons in 10–40% centrality Au+Au collisions. These results suggest that charm quarks have achieved local thermal equilibrium with the medium created in such collisions.

The energy dependent measurements reported here will be enhanced after STAR acquires greatly increased statistics using upgraded detectors in Phase-II of the RHIC Beam Energy Scan (BES-II).

2 Heavy flavor production

The excellent HFT resolution enabled study of charmed hadrons with even smaller decay lengths than D^0, in particular Λ_c. Figure 3 shows the reconstructed invariant mass of $pK\pi$ in 10–60% Au+Au collisions at $\sqrt{s_{NN}}$ = 200 GeV, with topological cuts optimized for Λ_c. A peak at the Λ_c mass is observed clearly. STAR has performed the first measurements of centrality dependence of Λ_c production in heavy ion-collisions. It was found that Λ_c/D^0 ratio increases from peripheral to central, which indicates hot medium effects. The measured STAR data point was compared to model calculations with various levels of charm quark thermalization in the medium and different coalescence implementations of the coalescence mechanism.

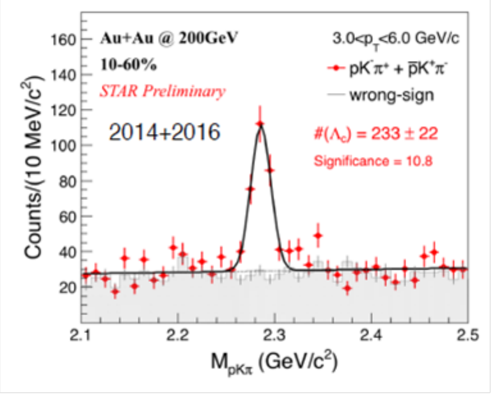

Figure 3. Reconstructed invariant mass of $pK\pi$ for 10-60% centrality Au+Au collisions from run years 2014 and 2016, representing signal of Λ_c baryons.

Energy loss of charm and bottom quarks is of great interest since quarks are expected to exhibit different radiative energy loss depending on their mass. The nuclear modification factor $R_{AA}(p_T) = \sigma_{in}^{pp} / < N_{coll}^{AA} > \cdot [d^2N_{AA}/dp_T d\eta]/[d^2\sigma_{pp}/dp_T d\eta]$ of inclusive J/ψ via the di-muon channel at midrapidity in 0-40% Au+Au collisions at $\sqrt{s_{NN}}$ = 200 GeV was compared to LHC results [7]. The strong suppression at high p_T obtained at RHIC indicates significant J/ψ dissociation.

STAR has shown Υ R_{AA} for the $2S + 3S$ states for Au+Au collisions at $\sqrt{s_{NN}} = 200$ GeV as a function of particles number N_{part}, compared to CMS data. There are indications that the suppression is weaker at $\sqrt{s_{NN}} = 200$ GeV than at $\sqrt{s_{NN}} = 2.76$ TeV, which might be due to the lower temperature at RHIC. Weaker suppression of the 1S state compared to the 2S+3S states in central collisions is consistent with the picture of sequential melting.

3 Global polarization measurements

STAR has recently reported measurements of global Λ polarization in Au+Au collisions [8, 9]. The existence of an alignment between the angular momentum of a non-central collision and the spin of emitted particles was demonstrated for the first time, revealing that the fluid produced in heavy-ion collisions is by far the most vortical system ever observed. The measured effect for Λ and $\bar{\Lambda}$ hyperons show a positive polarization of the order of a few percent for energies of BES and of tens of percent for highest RHIC energy. The signal increases with decreasing collision energy, and a systematic splitting between Λ and $\bar{\Lambda}$ is observed which might indicate an additional magnetic component.

Spin-orbit coupling can generate a spin alignment, or polarization, along the direction of the vorticity which is on average parallel to the overall angular momentum of the system. Figure 4 shows the measured global polarization of Λ and $\bar{\Lambda}$ as a function of the collision energy for the 20–50% centrality bin in Au+Au collisions. A set of different theoretical models is argued to describe the measured polarization [10]-[12].

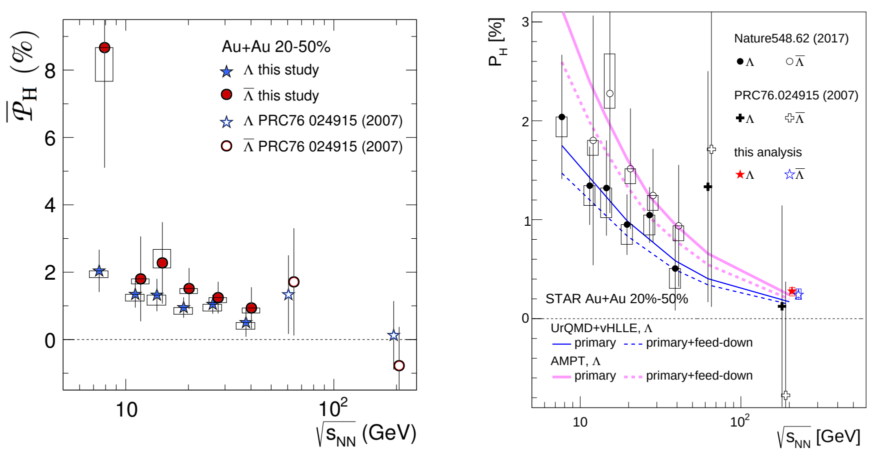

Figure 4. Global polarization $\bar{P}_H$ (where H = Λ or $\bar{\Lambda}$) of Λ and $\bar{\Lambda}$ as a function of the collision energy $\sqrt{s_{NN}}$ for 20-50% centrality Au+Au collisions. **Left.** The results of the measurements for BES energy range ($\sqrt{s_{NN}} < 40$ GeV) are compared with the data previously calculated for 62.4 and 200 GeV collisions, for which only statistical errors are plotted. Boxes indicate systematic uncertainties. **Right.** Thin lines show calculations from a (3+1)D cascade + viscous hydrodynamic model (UrQMD+vHLLE) [10] and bold lines show the AMPT model calculations [11]. In the case of each model, primary Λ with and without the feed-down effect are indicated by dashed and solid lines, respectively. Open boxes and vertical lines show systematic and statistical uncertainties, respectively. Data points at 200 GeV and for $\bar{\Lambda}$ are slightly horizontally shifted for visibility.

Calculations for primary Λ and all Λ taking into account the effect of feed-down, from a (3+1)D viscous hydrodynamic model vHLLE with the UrQMD initial state [10] are shown for comparison. The model calculations agree with the data over a wide range of collision energy, including $\sqrt{s_{NN}}$ = 200 GeV within the current accuracy of experimental measurements. Calculations from a Multi-Phase Transport (AMPT) model [11] predict slightly higher polarization than the hydrodynamic model, but are also in good agreement with the data within uncertainties.

Figure 5 shows differential measurements of the polarization, versus the collision centrality, and hyperons transverse momentum. With the given large uncertainties, it is not clear if the polarization saturates or even starts to drop off in the most peripheral collisions (Fig. 5, left). The polarization dependence on p_T is weak or absent (Fig. 5, right), considering the large uncertainties, which is consistent with the expectation that the polarization is generated by a rotation of the system. No significant dependence on pseudorapidity or transverse momentum was observed. The statistical uncertainties need to be improved to reach a definitive conclusion on the event-by-event charge asymmetry, which is consistent with a possible contribution to the global polarization from the axial current induced by the initial magnetic field.

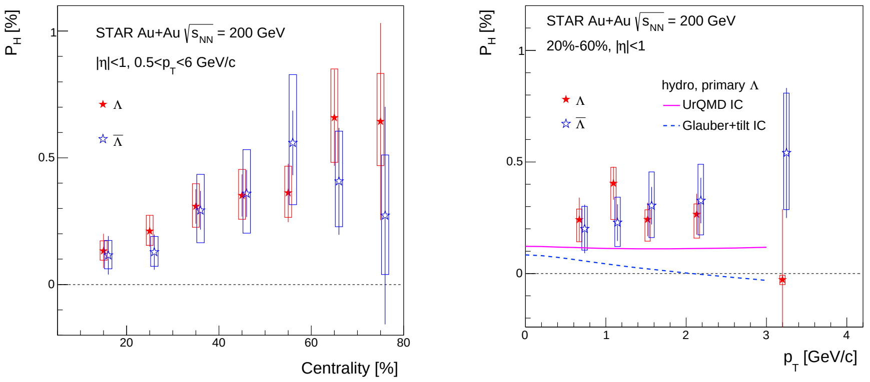

Figure 5. Left. Polarization of Λ and $\bar{\Lambda}$ as a function of the collision centrality in Au+Au collisions at $\sqrt{s_{NN}}$ = 200 GeV. **Right.** Polarization of Λ and $\bar{\Lambda}$ as a function of transverse momentum p_T for the 20 – 60% centrality bin in Au+Au collisions at $\sqrt{s_{NN}}$ = 200 GeV. Hydrodynamic model calculations for Λ with two different initial conditions are compared. Open boxes and vertical lines show systematic and statistical uncertainties. Data points for $\bar{\Lambda}$ are slightly shifted for visibility.

4 Results from fixed-target program

STAR has demonstrated the capability to operate at very low $\sqrt{s_{NN}}$ = 4.5 GeV in the fixed-target mode. A test run with Au-target installed 2m from the TPC center within the beam pipe was done recently. During 3 minutes run 1M events of 0-30% centrality Au+Au were recorded. Figure 6 shows energy dependence of measured directed flow slope parameter $dv_1/dy|_{y=0}$, comparing the data from fixed-target mode to BES STAR [13] and AGS results [14]. Within the uncertainties the data are consistent with those measured in a collider experiments. Fig. 6, left, shows the slope parameter for lightest mesons ($\pi^{\pm}$, $K^{\pm}$ and K_S^0) and Fig. 6, right, the same for lightest baryons (p, Λ and $\bar{p}$).

Figure 7 demonstrates STAR capabilities for particle identification in fixed-target regime for strange particles. Spectra are plotted in dependence of transverse kinetic energy for K_S^0, left, and Λ, right.

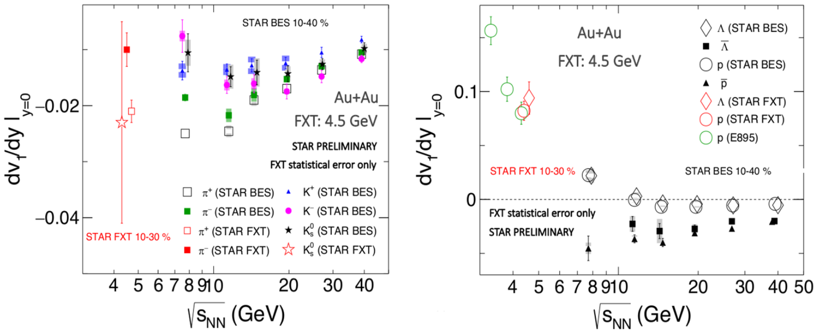

Figure 6. Directed flow slope at mid-rapidity as a function of the center-of-mass energy $\sqrt{s_{NN}}$ for the STAR fixed-target data. **Left**: $dv_1/dy|_{y=0}$ for light mesons, compared to results obtained at STAR BES-I. **Right**: $dv_1/dy|_{y=0}$ for light baryons, compared to results obtained at AGS and STAR BES-I.

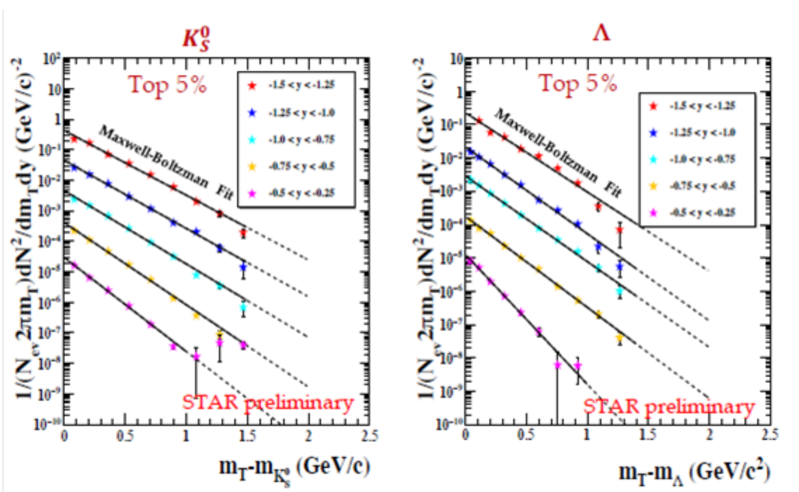

Figure 7. Spectra of strange particles obtained in fixed-target mode as a function of transverse kinetic energy. **Left**: Spectra of K^0_S. **Right**: Spectra of Λ.

5 Hypertriton lifetime measurements

STAR has performed a precise measurement of the ${}^{3}_{\Lambda}H$ and ${}^{3}_{\bar{\Lambda}}\bar{H}$ lifetime. Mesonic decay modes were used to reconstruct ${}^{3}_{\Lambda}H$ from Au+Au collisions data. All ${}^{3}_{\Lambda}H$ measurements, regardless of beam energy, were combined to increase the statistics. The hypertriton candidates were reconstructed from the invariant mass distributions of the daughters: ${}^{3}He + \pi^-$ for the 2-body, and $d + p + \pi^-$ for the 3-body decay channel of ${}^{3}_{\Lambda}H$ and ${}^{3}\bar{He} + \pi^+$ for the 2-body, and $\bar{d} + \bar{p} + \pi^+$ for the 3-body decay channel for ${}^{3}_{\Lambda}H$ and ${}^{3}_{\bar{\Lambda}}\bar{H}$, respectively.

A minimum χ^2 estimation is used to determine the lifetime of $\tau = 142 + 24 - 21(stat.) \pm 31(syst.)$ ps. This lifetime is about 50% shorter than the lifetime $\tau = 263 \pm 2$ ps of a free Λ, indicating strong hyperon-nucleon interaction in the hypernucleus system. Figure 8 shows the experimentally measured hypertriton lifetime.

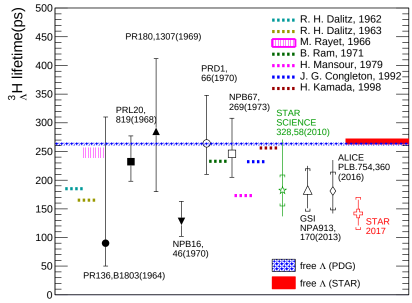

Figure 8. A summary of worldwide ${}^{3}_{\Lambda}H$ lifetime experimental measurements and theoretical calculations. The two star markers are the STAR results published in 2010 and in 2018.

The STAR experiment will collect large datasets for Au+Au collisions during BES phase II in years 2019-2020, which will further reduce experimental uncertainties on the ${}^{3}_{\Lambda}H$ lifetime and will likely provide new insight into it structure.

6 Detector upgrades for BES-II

BES phase II, planned to run in years 2019 and 2020, covers the energy range $\sqrt{s_{NN}} < 20$ GeV in both collider and fixed-target mods. The primary goals of BES-II are the search for the QCD critical point and for signatures of a phase transition between hadronic gas and QGP phases. In order to increase detector acceptance and particle identification capabilities, three major subsystem upgrades were proposed and to be ready till the end of 2018: Event Plane Detector (EPD), the inner TPC upgrade (iTPC) and the endcap Time-Of-Flight detector (eTOF). The EPD was fully installed and became operational for run year 2018, replacing the Beam-Beam Counter (BBC) as a minimum-bias trigger detector. EPD allows forward measurements of both centrality and event plane determination reducing systematic uncertainty due to autocorrelations for midrapidity analysis. This new detector consists of two disks that are placed on both sides of the STAR detector. EPD has pseudorapidity acceptance of $2.1 < |\eta| < 5.1$ with 16 radial segments and 24 azimuthal segments.

The iTPC will increase the acceptance of the TPC up to $|\eta| = 1.5$ increasing number of readout pad rows from 13 to 40 and maximum number of hits per track from 45 to 72. It will improve the dE/dx resolution, and will allow tracks to be reconstructed down to p_T of 60 MeV/c. A single inner sector was installed for tests for run year 2018 and the full complement of 24 will be installed for run year 2019.

The eTOF will be installed on one side of STAR, which will extend PID capabilities at forward rapidity. Three modules of eTOF were installed behind one of the TPC sectors for run year 2018 and the full complement of 36 will be installed for run year 2019. Combining all three detector systems will reduce significantly the systematic uncertainties of many observables and improve the statistical precision of STAR BES measurements.

7 Summary

STAR has presented a variety of experimental results in wide energy range $\sqrt{s_{NN}}$ from 4.5 GeV to 200 GeV obtained in the fixed-target and collider mode. Systematic study of collision energy dependence of strange particles indicates the constituent quark coalescence. Results on heavy flavor production measured with HFT include directed and elliptic flow of D^0 mesons and reconstruction of Λ_c baryons, which supports the idea of charm thermalization at RHIC energies. Global Λ polarization measurements in Au+Au collisions previously made for the energies of the BES now has been presented revealing a non-zero effect for the highest RHIC energy 200 GeV. These observations can provide new insight on the vorticity in heavy-ion collisions. Three detector upgrades are expected to be ready prior to the run year 2019 for the upcoming Beam Energy Scan phase II. The iTPC, eTOF and EPD detectors will improve the acceptance, particle identification capabilities, and reduce systematic uncertainties for many observables.

References

[1] S. Voloshin and Y. Zhang, Z. Phys. C **70**, 665 (1996)
[2] L. Adamczyk *et al.* [STAR Collab.], Phys. Rev. Lett. **120**, 062301 (2018)
[3] L. Adamczyk *et al.* [STAR Collab.], Phys. Rev. Lett. **112**, 162301 (2014)
[4] J. C. Dunlop, M. A. Lisa and P. Sorensen, Phys. Rev. C **84**, 044914 (2011).
[5] H. Qiu [STAR Collab.], Nucl. Phys. A **931**, 1141 (2014)
[6] L. Adamczyk *et al.* [STAR Collab.], Phys. Rev. Lett. **118**, 212301 (2017)
[7] B. B. Abelev *et al.* [ALICE Collab.], Phys. Lett. B **734**, 314 (2014)
[8] L. Adamczyk *et al.* [STAR Collab.], Nature **548**, 62 (2017)
[9] J. Adam *et al.* [STAR Collab.], Phys. Rev. C **98**, 014910 (2018)
[10] I. Karpenko and F. Becattini, Eur. Phys. J. C **77**, 213 (2017)
[11] H. Li, L. G. Pang, Q. Wang and X. L. Xia, Phys. Rev. C **96**, 054908 (2017)
[12] O. Rogachevsky, A. Sorin and O. Teryaev, Phys. Rev. C **82**, 054910 (2010)
[13] L. Adamczyk *et al.* [STAR Collab.], Phys. Rev. Lett. **112**, 162301 (2014)
[14] H. Liu *et al.* [E895 Collab.], Phys. Rev. Lett. **84**, 5488 (2000)
[15] L. Adamczyk *et al.* [STAR Collab.], Phys. Rev. C **97**, 054909 (2018)